

Bond mechanism of 18-mm prestressing strands: New insights and design applications

Canh N. Dang^{1,2a}, José R. Martí-Vargas^{*3} and W. Micah Hale^{4b}

¹Department for Management of Science and Technology Development, Ton Duc Thang University, Ho Chi Minh City, Vietnam

²Faculty of Civil Engineering, Ton Duc Thang University, Ho Chi Minh City, Vietnam

³Institute of Concrete Science and Technology (ICITECH), Universitat Politècnica de València, 4G, Camino de Vera s/n, 46022 Valencia, Spain

⁴University of Arkansas, Department of Civil Engineering, 4190 Bell Engineering Center, Fayetteville, AR 72701, USA

(Received December 2, 2019, Revised May 3, 2020, Accepted May 18, 2020)

Abstract. Pretensioned concrete (PC) is widely used in contemporary construction. Bond of prestressing strand is significant for composite-action between the strand and concrete in the transfer and flexural-bond zones of PC members. This study develops a new methodology for quantifying the bond of 18-mm prestressing strand in PC members based on results of a pullout test, the Standard Test for Strand Bond (STSB). The experimental program includes: (a) twenty-four pretensioned concrete beams, using a wide range of concrete compressive strength; and (b) twelve untensioned pullout specimens. By testing beams, the transfer length, flexural-bond length, and development length were all measured. In the STSB, the pullout forces for the strands were measured. Experimental results indicate a significant relationship between the bond of prestressing strand to the code-established design parameters, such as transfer length and development length. However, the code-predictions can be unconservative for the prestressing strands having a low STSB pullout force. Three simplified bond equations are proposed for the design applications of PC members.

Keywords: pretensioned concrete; prestressing strand; bond; transfer length; development length; STSB; design application

1. Introduction

In pretensioned concrete (PC) members, concrete and prestressing strands work as a composite material. For the prestressing strands, the known mechanical properties typically include yield strength, elongation, and breaking strength. These properties are significant in carrying the prestress force or tensile stress as PC members resist external loads. ASTM (2018) specifies the minimum requirements for the mechanical properties of 9.5-mm to 18-mm strands. On the other hand, as in other cases with different materials developing a composite action (Barakat *et al.* 2019; Tang 2018), the bond property is critical for composite action between the prestressing strands and concrete. ASTM (2015) describes a pullout test, technically termed as Standard Test for Strand Bond (STSB), to determine the bond of an untensioned prestressing strand. However, the test has no official minimum requirement for the bond strength.

The bond of prestressing strand can vary between strand manufacturers. In addition, the transportation and storage conditions at construction sites of the strands can affect the

strand bond, since the bond depends on the surface characteristics of the prestressing strand (Osborn *et al.* 2008). In a PC member, the bond of prestressing strand differs for different stages of prestress which, in turn, relate to two significant design parameters of PC members (Buckner 1995): transfer length (or transmission length) and development length (or anchorage length), the latter including the former and the flexural-bond length. The bond in the transfer zone is necessary to transfer the strand stress to the adjacent concrete. The bond in the flexural-bond zone is needed for the strand to develop the ultimate stress at the nominal flexural capacity. The bond in the flexural-bond zone relies on the mechanical interlock between the prestressing strand and concrete, similar to the performance of deformed reinforcement. The bond in the transfer zone is additionally contributed by the Hoyer's effect (Janney 1954); a friction at the interface of prestressing strand and concrete, generated as the hardened concrete restrains the strand's transverse expansion. The adhesion, a kind of chemical bond between prestressing strand and concrete, is present in both zones, but its contribution to the strand bond is minimal (Russell and Burns 1993). The following equations express this conception:

$$f_b = f_{b,Hoyer} + f_{b,mech} \quad (\text{in transfer zone}) \quad (1a)$$

$$f_b = f_{b,mech} \quad (\text{in flexural-bond zone}) \quad (1b)$$

While mechanical interlock depends on the strand surface condition, the Hoyer's effect varies over time as it is

*Corresponding author, Ph.D., Professor
E-mail: jrmarti@cst.upv.es

^a Ph.D. Researcher
E-mail: canhdang@tdtu.edu.vn

^b Ph.D. Professor
E-mail: micah@uark.edu

affected by concrete creep and shrinkage (Barnes *et al.* 2003). The difference in these bond mechanisms is a source of complexities in the prediction of bond in PC members. In this paper, a new methodology to simplify the prediction of strand bond in PC members using results from STSB is presented. The experimental data and presented observations are significant to recognize the influence of the bond of prestressing strands to code-established design parameters, and provide insights to the bond mechanisms.

2. Literature review

An extensive effort has been made to develop applicable techniques for investigating the bond of prestressing strands (Abrishami and Mitchell 1993; Bai and Davidson 2016; Martí-Vargas *et al.* 2014a, b; Oh *et al.* 2014; Jiang *et al.* 2017; Warenycia *et al.* 2017). An analytical bond stress-slip model can represent the complex interaction between the prestressing strand and the concrete in the transfer zone (Balazs 1992; Dang *et al.* 2015; Martí-Vargas *et al.* 2014c; Park and Cho 2014; Ortega *et al.* 2019). This model can also be used for estimating transfer length (Den Uijl 1998; Dang *et al.* 2016b; Lee *et al.* 2017; Motwani and Laskar 2019). However, the model typically consists of several nonlinear second-order differential equations, so its application is not straightforward (Balazs 1992; Den Uijl 1998; Dang *et al.* 2015; Kareem *et al.* 2019; Ramirez-Garcia *et al.* 2017).

With recent developments in finite-element programs, like ANSYS or ABAQUS, modelling a single or multiple-strand PC element is possible. Nonlinear finite elements are used to represent the concrete, prestressing strand, and the bond between the two materials. The developed finite-element models can capture the variation in the stress in prestressing strand or tension-compression stress in concrete, or simulate micro-cracks adjacent to the prestressing strand (Arab *et al.* 2011; Yapar *et al.* 2015; Abdelatif *et al.* 2015; Llau *et al.* 2016; Warenycia *et al.* 2017; Steensels *et al.* 2017; Van Meirvenne *et al.* 2018). However, the computational effort is extensive, both in preparing the finite-element models as well as running analysis and post-processing results. Therefore, the efficiency and adaptability of those models in design applications are reduced.

In addition, concrete creep and shrinkage are influential factors to the Hoyer's effect. It should be noted that the concrete deformation under the expansion of prestressing strands is independent to the deformation in the longitudinal direction of PC members. Therefore, it is required to place specific finite concrete elements around the prestressing strands to represent the concrete behavior under the sustained compressive stresses generated by the expansion of the strands after release. The concrete deformation relaxes the constrained prestressing strands and reduces the bearing pressure generated by the Hoyer's effect. In the literature, there is limited research into the effect of transverse concrete creep and shrinkage to the strand bond, but the increase in transfer length over time is a clear evidence of this effect (Barnes *et al.* 2003; Caro *et al.* 2013; Dang *et al.* 2016b).

With respect to mechanical interlock, the helical shape of a 7-wire prestressing strand offers a significant contribution. As the strand is in tension, the six outer wires tend to twist around the center wire and slip in the applied-force direction. At the same time, the hardened concrete resists the effects associated to the slip of these wires. Using pullout tests is an efficient way to evaluate the strand bond generated by the mechanical interlock. The embedment length should be longer than one pitch of the strand, typically varying from $8d_b$ to $12d_b$, to prevent the strand sample from free-twisting, where d_b is the strand diameter (Den Uijl 1998). Several pullout test setups have been developed, such as the Moustafa Test (Moustafa 1974), the Post-Tensioning Institute (PTI) Bond Test, the North American Strand Producers (NASP) (Russell 2006), and the STSB (Ramirez and Russell 2008; ASTM 2015). STSB is performed by pulling an untensioned strand sample from a steel casing filled with mortar. The bond of prestressing strand can be computed using Eq. (2).

$$f_{b,STSB} = \frac{\text{Pullout_Force}}{C_p \times L_{\text{embedment}}} \quad (2)$$

With a number of complexities regarding the magnitude and the changes in the Hoyer's effect over time and the variation in strand surface condition, it is necessary to develop a simple technique to quantify the two main bond components: the Hoyer's effect and the mechanical interlock. The utilization of the STSB is a feasible approach as it is a reliable pullout test and able to fully capture the bond generated by the mechanical interlock (Dang *et al.* 2014a). In addition, STSB is a recommended Quality Control (QC) test by various organizations such as American Society for Testing and Materials (ASTM) and International Federation for Structural Concrete (FIB).

3. Design code provisions

The current design codes specify equations to calculate transfer length (L_t) and development length (L_d). In the development-length equation, the first term represents for the transfer length, and the second term represents for the flexural-bond length (L_{flexural}). The bond strength in each zone (transfer zone and flexural-bond zone) is derived from Eq. (3) by using the corresponding bond length ($L_{\text{embedment}}$).

$$f_b = \frac{f_p \times A_p}{C_p \times L_{\text{embedment}}} \quad (3)$$

3.1 Building Code Requirements for Structural Concrete (ACI 318-19)

ACI 318-19 (ACI 2019) provides two equations to calculate transfer and development length as shown in Eqs. (4a)-(4b), respectively. Using Eq. (3), the bond equations in the transfer zone and flexural-bond zone are shown in Eqs. (4c)-(4d), with the computed bond strengths of 3.02 MPa and 1.01 MPa, respectively. These equations indicate that

ACI 318-19 bond strengths are independent from the concrete strength and strand surface condition, regardless of the number of studies that have shown the influence of these factors to bond strength (Mitchell *et al.* 1993; Martí-Vargas *et al.* 2013; Dang *et al.* 2014b; Riding *et al.* 2016).

$$L_t = \frac{1}{20.7} f_{pe} d_b \quad (4a)$$

$$L_d = \frac{1}{20.7} f_{pe} d_b + \frac{1}{6.9} (f_{ps} - f_{pe}) d_b \quad (4b)$$

$$f_b = \frac{f_{pe} \times A_p}{C_p \times L_t} \quad (\text{in transfer zone}) \quad (4c)$$

$$f_b = \frac{(f_{ps} - f_{pe}) \times A_p}{C_p \times L_{flexural}} \quad (\text{in flexural-bond zone}) \quad (4d)$$

3.2 Load and Resistance Factor Design – Specifications for Highway Bridges (AASHTO-LRFD)

The American Association of State Highway and Transportation Officials (AASHTO) provides an alternative equation for determining the development length for PC members with a depth greater than 610 mm (AASHTO 2017, Section 5.11.4). When compared to ACI 318-19 [Eq. (4b)], the AASHTO-LRFD equation scales up the development length by 60% to account for the shear effect in deep PC members. For the members with a depth less than or equal to 610 mm, the AASHTO-LRFD and ACI 318-19 development-length equations are identical.

3.3 Eurocode 2 – Design of Concrete Structures (EC2)

EC2 (CEN 2004) provides equations to calculate the transmission length (technically similar to the transfer length) and anchorage length (technically similar to the development length), as shown in Eqs. (5a)-(5b), respectively. The design values of the bond strength are shown in Eqs. (5c)-(5d).

$$L_t = \alpha_1 \alpha_2 d_b \frac{\sigma_{pi}}{f_{bpt}} \quad (\text{average value}) \quad (5a)$$

$$L_d = 1.2L_t + (\alpha_2 d_b) \left(\frac{\sigma_{pd} - \sigma_{pe}}{f_{bpd}} \right) \quad (5b)$$

$$f_{bpt} = \eta_{p1} \eta_1 f_{ctd,R} \quad (5c)$$

$$f_{bpd} = \eta_{p2} \eta_1 f_{ctd,28} \quad (5d)$$

Eq. (5a) is used to compute an average transmission length. In structural design, a short transmission length can be an issue when checking concrete stresses at release, and

a long transmission length can be an issue at service loads when the moment and shear capacity are considered. Therefore, EC2 further includes two coefficients of 0.8 and 1.2 to Eq. (5a) for these considerations, respectively. With an emphasis on a 7-wire prestressing strand ($\alpha_2 = 0.19$, $\eta_{p1} = 3.2$ and $\eta_{p2} = 1.2$), with a good bond condition ($\eta_1 = 1.0$) and that is gradually released ($\alpha_1 = 1.0$), the bond strength in the transfer zone is computed as shown in Eqs. (5e)-(5f). It should be noted that the bond at release is 50% higher than the bond at service due to the adjustment of the two coefficients (0.8 and 1.2). Similarly, the bond strength in the flexural-bond zone is shown in Eq. (5g). When compared to the ACI 318-19 bond equations above, the EC2 bond equations additionally include the effect of concrete tensile strength. Therefore, the use of high-strength concrete is expected to shorten transmission and anchorage length.

$$f_b = 3.0 f_{ctd,R} \quad (\text{in transfer zone at release}) \quad (5e)$$

$$f_b = 2.0 f_{ctd,R} \quad (\text{in transfer zone at 28 days of age}) \quad (5f)$$

$$f_b = 0.9 f_{ctd,28} \quad (\text{in flexural-bond zone}) \quad (5g)$$

3.4 Model Code for Concrete Structures 2010 (MC 2010)

MC 2010 (FIB 2013) provides two equations to compute transmission length and anchorage length, as shown in Eqs. (6a)-(6b), respectively, with the design bond value shown in Eq. (6c).

$$L_t = \alpha_{p1} \alpha_{p2} \alpha_{p3} \left(\frac{7}{36} d_b \right) \frac{\sigma_{pi}}{f_{bpd}} \quad (6a)$$

(average value with $\alpha_{p2} = 0.75$)

$$L_d = 1.33L_t + \left(\frac{7}{36} d_b \right) \left(\frac{\sigma_{pd} - \sigma_{pe}}{f_{bpd}} \right) \quad (6b)$$

$$f_{bpd} = \eta_{p1} \eta_{p2} f_{ctd} \quad (6c)$$

The coefficient α_{p2} considers the design states to be verified. A value of 1.0 is used for calculating anchorage length when the moment and shear capacity are considered. A value of 0.5 is used for verifying transverse stresses due to the development and distribution of prestress in the anchorage zone. A value of 0.75 was established to obtain an average value, which is also consistent with EC2 transmission length formulation (Martí-Vargas *et al.* 2007). Accordingly, two coefficients of 0.67 (0.5/0.75) and 1.33 (1.0/0.75) are used for estimating transmission length at release and at the service state (when the moment and shear capacity are considered), respectively. A coefficient of 1.33 is present in the first term of Eq. (6b) to scale up the predicted transmission length at the service state. With the same emphasis on a 7-wire prestressing strand as

aforementioned ($\alpha_{p1} = 1.0$; $\alpha_{p3} = 0.5$; $\eta_{p1} = 1.2$; and $\eta_{p2} = 1.0$), the bond equations in the transmission zone, shown in Eqs. (6d)-(6e), are slightly different from those of EC2 due to the discrepancy in the aforementioned coefficients. The bond equation in the flexural-bond zone, shown in Eq. (6f), is identical to the one of the EC2 [see Eq. (5g)].

$$f_b = 3.6f_{ctd,R} \quad (\text{in transfer zone at release}) \quad (6d)$$

$$f_b = 1.8f_{ctd,R} \quad (\text{in transfer zone at 28 days of age}) \quad (6e)$$

$$f_b = 0.9f_{ctd,28} \quad (\text{in flexural-bond zone}) \quad (6f)$$

4. Experimental investigation

4.1 Standard Test for Strand Bond (STSB)

Twelve strand samples were collected from a reel of prestressing strand, and equally divided into two groups (S1 and S2). Each strand sample was positioned at the center of a 450-mm long steel casing. Excluding 50-mm at the end for a bond breaker placement, the total embedded length of the strand sample was 400 mm (L_{embed} in Eq. 2). The steel casing was filled with mortar, which had a 24-hour compressive strength of 32 MPa and satisfied the limit of 31.0 to 34.5 MPa required by ASTM A1081 (ASTM 2015). The pullout force and strand slip were monitored continuously. The forces corresponding to a free-end slip of 0.25 mm and 2.5 mm were recorded as $P_{initial}$ and P_{final} , respectively, and summarized in Table 1. A STSB test setup is presented in Appendix 1.

Based on sample S2-1, Fig. 1 depicts a typical force-slip relationship. As shown in Fig. 1, the free-end slips 0.25 mm when the pullout force reaches 125 kN. The strand slip indicates that the bond stress has exceeded the bond strength generated by mechanical interlock. At this stage, additional and significant slips can be developed following a hardening evolution: up to 160 kN of pullout force (28% of increase over 125 kN) when free-end slips 2.5 mm (10 times higher than 0.25 mm). Therefore, from a conservative perspective, it is acceptable to consider the mechanical bond strength only up to the stage that the pullout force reaches $P_{initial}$, since in design a bond failure is considered brittle and abrupt and can cause a catastrophic failure of PC members (Naji *et al.* 2016).

4.2 Pretensioned concrete beam fabrication

Four concrete mixtures were developed, including: (i) normal-strength and high-strength conventional concrete (N-CC and H-CC); and (ii) normal-strength and high-strength self-consolidating concrete (N-SCC and H-SCC). The 1-day and 28-day compressive strengths ranged from 41 to 68 MPa and from 64 to 93 MPa, respectively, as summarized in Table 2. These mixtures were used to cast 24 pretensioned concrete beams, which were equally divided into 6 groups. The mixtures and concrete properties at the fresh state of these mixtures can be referred to Dang *et al.* (2016b).

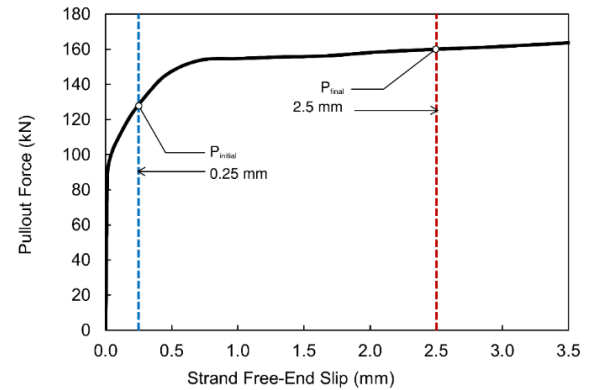


Fig. 1 Typical relationship between pullout force and strand free-end slip (sample S2-1)

The beam's dimensions were 165-mm wide, 305-mm deep, and 5500-mm long. One 18-mm prestressing strand, Grade 1860, was positioned at the center, 50-mm from the bottom fiber of the beam. The strand was tensioned to 75% of the nominal ultimate strength ($f_{pj} = 0.75 \times 1860 \text{ MPa} = 1395 \text{ MPa}$). The prestress was maintained during casting using hydraulic jacks and until prestress release, which was on average 24 hours after casting.

The prestress was gradually released by reducing the pressure in the hydraulic jacks, which is one of the cases specified in the design codes as aforementioned. Top reinforcement included two no.16 bars, placed at 50-mm from the top fiber of the beam to resist the tensile stresses at release. Shear reinforcement was comprised of closed-hoop stirrups, no.6 bars, 150-mm spacing. The reinforcement was designed based on the shear requirements for the flexure tests used to determine development length.

There were two beam groups that contained two prestressing strands (H-CC-D and H-SCC-D). The beam configuration and reinforcement detail were similar to the beams with one strand (H-CC-S and H-SCC-S), with a few adjustments. The two prestressing strands were placed at 50-mm center-to-center apart horizontally. Due to a larger prestress force, top reinforcement included two no.19 bars, and shear reinforcement was at 75-mm spacing. The testing procedure of H-CC-D and H-SCC-D beam groups was identical to the H-CC-S and H-SCC-S groups, respectively.

4.3 Measurement of transfer length

The principle of transfer-length determination was based on the change in longitudinal concrete strains. Before release, the concrete beam is in a stress-free state, while the strand is in tension. After release, the bottom fiber of the beam is in compression due to the transfer of the prestress force. A DEMEC gauge was used to measure the changes in concrete strains at different locations along the beam and at different ages (one measurement at release and the other one at 28 days of age). The 95% Average Maximum Strain (AMS) technique was used for transfer-length determination (Russell and Burns 1993). A detailed procedure is summarized in Appendix 2. The main experimental results are presented in Table 3.

Table 1 Pullout force summary

Sample	$P_{initial}$ (kN)	P_{final} (kN)	$P_{initial}/P_{final}$	$f_{b,STSB}$ (MPa)
Group S1				
S1-1	115	144	0.80	3.80
S1-2	127	169	0.75	4.20
S1-3	126	165	0.76	4.16
S1-4	131	159	0.82	4.33
S1-5	139	175	0.79	4.59
S1-6	144	172	0.84	4.76
Average	130.3	164.0	0.793	4.31
Standard deviation	9.4	10.3	0.03	0.31
Group S2				
S2-1	125	160	0.78	4.13
S2-2	127	152	0.84	4.20
S2-3	126	161	0.78	4.16
S2-4	131	164	0.80	4.33
S2-5	139	156	0.89	4.59
S2-6	144	159	0.91	4.76
Average	132.0	158.7	0.832	4.36
Standard deviation	7.1	3.8	0.05	0.24

Table 2 Testing matrix and design parameters

Beam designation ^[a]	Concrete	Strand group	f'_{ci} (MPa)	f'_c (MPa)	f_{pj} (MPa)	f_{pi} ^[b] (MPa)	f_{pe} ^[c] (MPa)	f_{ps} ^[d] (MPa)
N-CC-S	N-CC	S1	43.2	65.2	1395	1337.0	1256.5	1834.8
H-CC-S	H-SC	S1	63.4	92.7	1395	1346.9	1279.6	1840.3
H-CC-D	H-SC	S1	67.5	87.9	1395	1298.7	1211.0	1822.3
N-SCC-S	N-SCC	S2	41.0	63.5	1395	1335.5	1252.5	1833.4
H-SCC-S	H-SCC	S2	54.6	73.8	1395	1343.3	1272.0	1836.5
H-SCC-D	H-SCC	S2	54.6	71.6	1395	1288.8	1192.9	1807.2

^[a] = The first term represents for concrete type, and the last terms represent for the number of prestressing strand (for example, N-CC-S is the group of beams cast with normal-strength, conventional concrete and one prestressing strand, or H-SCC-D is the group of beams cast with high-strength, self-consolidating concrete and two prestressing strands); ^[b] = strand stress after release, in which the elastic-shortening loss is calculated using AASHTO-LRFD, Section 5.9.5; ^[c] = strand stress at service, in which the elastic-shortening and time-dependent losses are calculated using AASHTO-LRFD, Section 5.9.5; ^[d] = strand stress at nominal flexural strength of the PC member, which is calculated using strain compatibility technique as specified in ACI 318-19, Section 20.3.2.

4.4 Measurement of development length

To determine development length, several beams were tested in flexure with different embedment lengths. An iterative process is required. The initial embedment length (the location –from the nearest support– at which the load is placed during the flexure tests) can be based on the design codes or from research recommendations. Once a beam is tested in flexure, the embedment length is then decreased or increased based on the type of failure. If the beam fails in flexure, the embedment length at which the beam was tested is longer than the required development length. If a bond

failure occurs, then the embedment length was shorter than the development length. If a shear failure occurs, additional tests may be needed to verify the embedment length. For each beam group in Table 2, eight flexure tests were conducted iteratively. Additional details on measurement aspects are introduced in Appendix 3. The main experimental results are presented in Table 3.

The flexural-bond length can be determined analytically. It is the difference in the measured development length and transfer length. In this study, the flexure tests were performed at 28 to 30 days of age, and therefore, the 28-day transfer length can be used to determine the flexural-bond length, as presented in Table 3.

Table 3 Measured transfer length, flexural-bond length, and development length

Beam designation ^[a]	L_{tR} (mm) ^[a]	L_{t28} (mm) ^[a]	L_d (mm) ^[b]	$L_{flexural}$ (mm) ^[b]
N-CC-S	658	765	1219	454
H-CC-S	575	651	1067	416
H-CC-D	584	662	1143	481
N-SCC-S	712	786	1219	433
H-SCC-S	610	694	1067	373
H-SCC-D	665	710	1219	509

^[a] = refer to Dang *et al.* (2016b); ^[b] = refer to Dang *et al.* (2016a).

Table 4 Recommended acceptance criteria and experimental results

Strand diameter (mm)	Average pullout force of 6 samples (kN)	Minimum pullout force of an individual sample (kN)	Reference
13 (acceptance criteria)	≥ 47.3	≥ 40.5	Ramirez and Russell (2008)
15 (acceptance criteria)	≥ 56.7	≥ 48.6	Ramirez and Russell (2008)
18 (acceptance criteria)	≥ 66.2	≥ 56.7	Morcous <i>et al.</i> (2012)
18 (experimental results)	164.0	satisfied	Group S1 [see Table 1]
18 (experimental results)	158.7	satisfied	Group S2 [see Table 1]

5. Results and discussion

5.1 Bond strength of untensioned strand samples

The pullout forces P_{final} of the two strand groups used in the research program are similar (164.0 kN with a coefficient of variation of 6.3% for group S1, and 158.7 kN with a coefficient of variation of 2.4% for group S2). It should be noted that both ASTM A1081 -Article 1- (ASTM 2015) and MC 2010 -Article 5.3.5.6 Bond Characteristics-FIB (2013) recommend using the STSB/NASP as a QC test for prestressing strand. However, no acceptance criteria is specified to determine if the prestressing strand is suitable for use in pretensioned concrete applications.

Ramirez and Russell (2008) proposed acceptance criteria for 13 and 15-mm (0.5 and 0.6-in.) and Morcous *et al.* (2012) for 18-mm (0.7-in.) prestressing strands, as presented in Table 4. The proposed criteria establish the minimum pullout force of an individual strand sample and the average pullout force of six samples. For the strands used in this research program, the measured pullout force of an individual strand sample and also the set of 6 samples per group meet the proposed acceptance criteria. The average pullout force of the two strand groups (161.3 kN) is 144% greater than the proposed minimum threshold of 66.2 kN. The effect of the variation in pullout force on the design of PC members is discussed in detail in section 5.3. Design applications.

The bond strength of each sample was calculated with Eq. (2) using the $P_{initial}$ pullout force and the results are summarized in Table 1.

It should be noted that bond strength is nonlinear along the embedment length in STSB (Dang *et al.* 2014a). The bond strength at the free-end is slightly less than the bond strength at the loaded-end, because the strand sample is

free-twisting. However, the difference at the two ends is minimal as the pullout force reaches $P_{initial}$ (Dang *et al.* 2014a). As a result, $P_{initial}$ can be adopted to compute an average value for the bond strength along the embedment length. In addition, the ratios of $P_{initial}$ to P_{final} —which is the value used regarding the acceptance criteria—of the two strand groups are similar. Therefore, a representative ratio of 0.8 can be used to compute $P_{initial}$ from the average P_{final} of 161.3 kN ($P_{initial} = 0.8 \times P_{final} = 0.8 \times 161.3 \text{ kN} = 129.0 \text{ kN}$). Accordingly, an average bond strength value of 4.26 MPa is used for further investigation.

5.2 Bond strength comparisons

Table 5 summarizes the computed bond strength in the transfer zone and in the flexural-bond zone. For each beam group, the bond strength in the transfer zone is greater than the bond strength in the flexural-bond zone. For the transfer zone, the bond strength at release is greater than the bond strength at 28 days of age. The cause of these observations is addressed in the following discussions.

Regarding the types of concrete, there is no significant difference in the bond strength for the beams cast with conventional concrete or self-consolidating concrete. This finding is in agreement with the findings reported by Trejo *et al.* (2008) and Myers *et al.* (2012).

Fig. 2 presents the measured and predicted bond strength at release and the STSB bond strength. A greater predicted bond value results in a shorter predicted transfer length, which is conservative for checking concrete stresses at release. The EC2 provides a conservative and fairly close prediction to the measured values, which is 7% greater on average. The MC 2010 prediction is in a similar trend, with 29% greater than the measured values on average. The ACI

Table 5 Bond strength in transfer zone and flexural-bond zone calculated from experimental results

Beam designation	f_b in transfer zone, at release (MPa) ^[a]	f_b in transfer zone, at 28 day of age (MPa) ^[b]	f_b in flexural-bond zone (MPa) ^[c]
N-CC-S	5.2	4.2	3.2
H-CC-S	6.0	5.0	3.4
H-CC-D	5.7	4.7	3.2
N-SCC-S	4.8	4.1	3.4
H-SCC-S	5.6	4.7	3.9
H-SCC-D	4.9	4.3	3.1

^[a] = calculated using Eq. (4c), with the strand stress in Table 2 and measured transfer length L_{tR} in Table 3; ^[b] = calculated using Eq. (4c), with the strand stress in Table 2 and measured transfer length L_{t28} in Table 3; ^[c] = calculated using Eq. (4d), with the strand stress presented in Table 2 and measured flexural-bond length $L_{flexural}$ presented in Table 3.

318-19 is not applicable for this kind of comparison as this code provides an in-service prediction of transfer length (not at release). The measured bond strength is approximately 25% greater than the STSB bond strength. The observation is reasonable, as the measured bond strength is affected by both the Hoyer's effect and mechanical interlock, while only the second factor contributes to the bond strength in the STSB.

Fig. 3 presents the measured and predicted bond strength at 28 days of age and the STSB bond strength. Contrary to the bond strength at release, a smaller predicted bond value results in a longer predicted transfer length, which is conservative for checking the shear strength of PC members and the development length of prestressing strands. Among the evaluated design codes, ACI 318-19 provides the most conservative prediction, which is 33% lower on average when compared to the measured values. EC2 and MC 2010 follow the same trend as ACI 318-19 with 14% and 23% lower in bond strength, respectively. The measured bond strength, on the other hand, is 5% greater than the STSB bond strength. This observation indicates a reduction in the bond between the prestressing strands and the concrete in PC members. As previously investigated by Barnes *et al.* (2003), concrete creep and shrinkage are dominant factors contributing to the bond reduction. The Hoyer's effect is the main contributor, as its mechanism relies on the bearing pressure generated by the prestressing strands to the adjacent concrete. The bond generated by mechanical interlock, however, can be physically maintained. The mechanical-interlock mechanism relies on the helical shape of prestressing strands, similar to the rib shapes in reinforcing bars.

Fig. 4 presents the measured and predicted bond strength in the flexural-bond zone and the STSB bond strength. With a principle similar to the bond strength in the transfer zone at 28 days of age, the current design codes provide a conservative prediction to the measured values with various degrees. On average, the predicted bond strengths by EC2, MC 2010, and ACI 318-19 are 41%, 41%, and 70% less than the measured values, respectively. The measured bond strength, however, is about 80% of the

STSB value. In other words, the mechanical-interlock bond in the flexural-bond zone of PC members is less than the STSB bond strength.

When a PC member reaches its nominal flexural strength, the prestressing strand in the flexural-bond zone is loaded at both ends; f_{pe} at the beginning of the zone and f_{ps} at the end of the zone. The values of f_{pe} and f_{ps} are summarized in Table 2. The strand diameter decreases accordingly due to the Poisson's effect when compared to the helical shape formed by the adjacent hardened concrete. The reduction in strand diameter can be numerically determined using Eq. 4 in Briere *et al.* (2013). In addition, the concrete adjacent to the prestressing strand can be in a damaged condition to a certain level due to elastic shortening. In the STSB, the prestressing strand sample is only loaded at one end; and therefore, the Poisson's effect is minimal. Therefore, there is no such concrete damage as in a PC member, which results in a greater bond strength.

5.3 Design applications

Table 6 shows a set of proposed equations for the bond of prestressing strand at different states, based on the bond strength determined from the STSB. The STSB pullout force can be directly accounted for when determining the transfer length and flexural-bond length. In the transfer zone, the bond strength of the prestressing strand at release is 25% higher than the STSB bond strength. At 28 days of age, the bond strength of the prestressing strand is 5% higher than the STSB bond strength. The increase in bond strength can be attributed to the Hoyer's effect, which is present along the transfer zone of PC members but not in the STSB. On average, the contribution of the Hoyer's effect to the bond of prestressing strand in the transfer zone of a PC member can be quantified by subtracting the $f_{b,STSB}$ component from the bond strength as shown in Table 6. In the flexural-bond zone, the bond of prestressing strand is 20% lower than the STSB value due to Poisson's effect and the potentially damaged concrete adjacent to the prestressing strand as aforementioned.

Alternatively, the bond of the prestressing strand in the transfer zone can be broken down into two components to separate the contribution of the mechanical interlock and Hoyer's effect, as shown in Table 6. The denominator "32

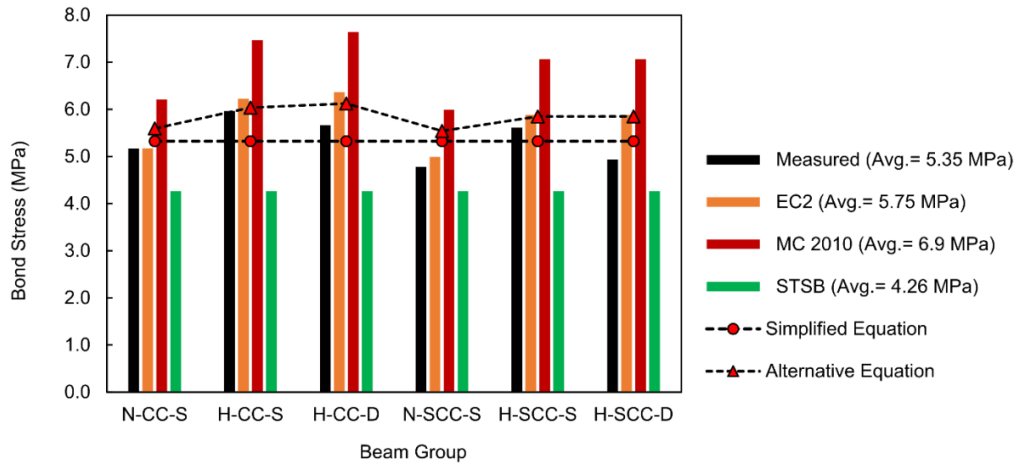


Fig. 2 Bond stress in transfer zone at release
 (Notes: The EC2 and MC 2010 bond strengths are calculated using Eqs. (5e)-(6d), respectively;
 The average STSB bond strength is derived from Table 1)

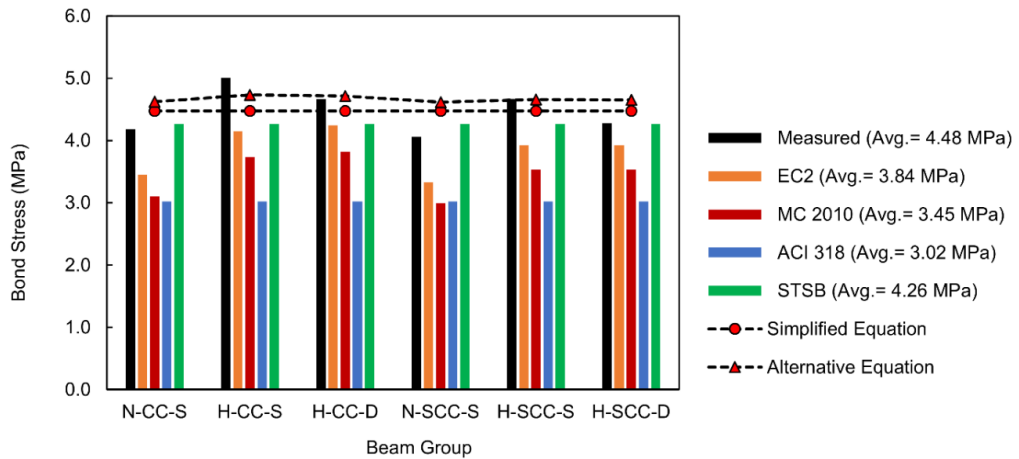


Fig. 3 Bond stress in transfer zone at 28 days of age
 (Notes: EC2, MC 2010 and ACI 318-19 bond strengths are calculated using Eqs. (5f)-(6e)-4(c), respectively;
 The average STSB bond strength is derived from Table 1)

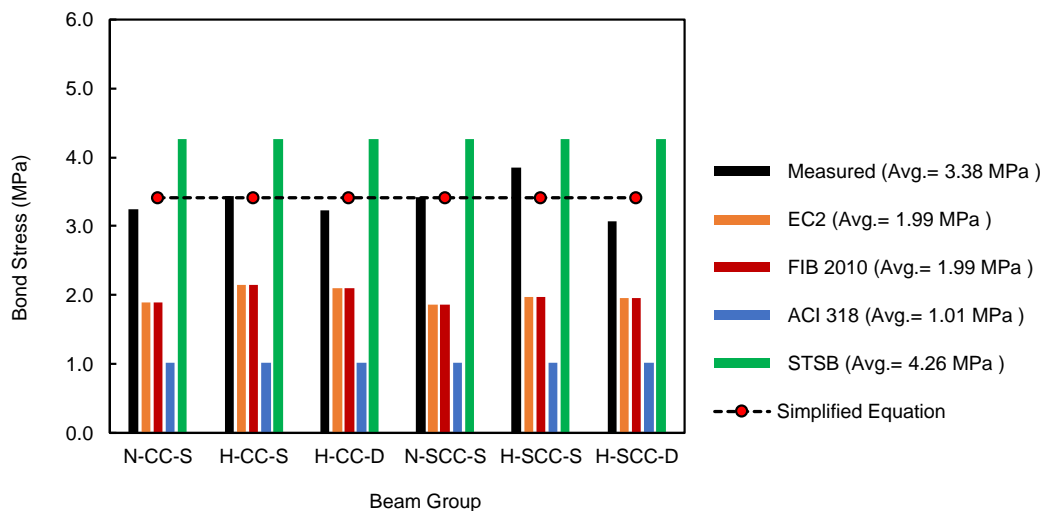


Fig. 4 Bond stress in flexural-bond zone
 (Notes: EC2, MC 2010 and ACI 318-19 bond strengths are calculated using Eqs. (5g)-(6f)-4(d), respectively;
 The average STSB bond strength is derived from Table 1)

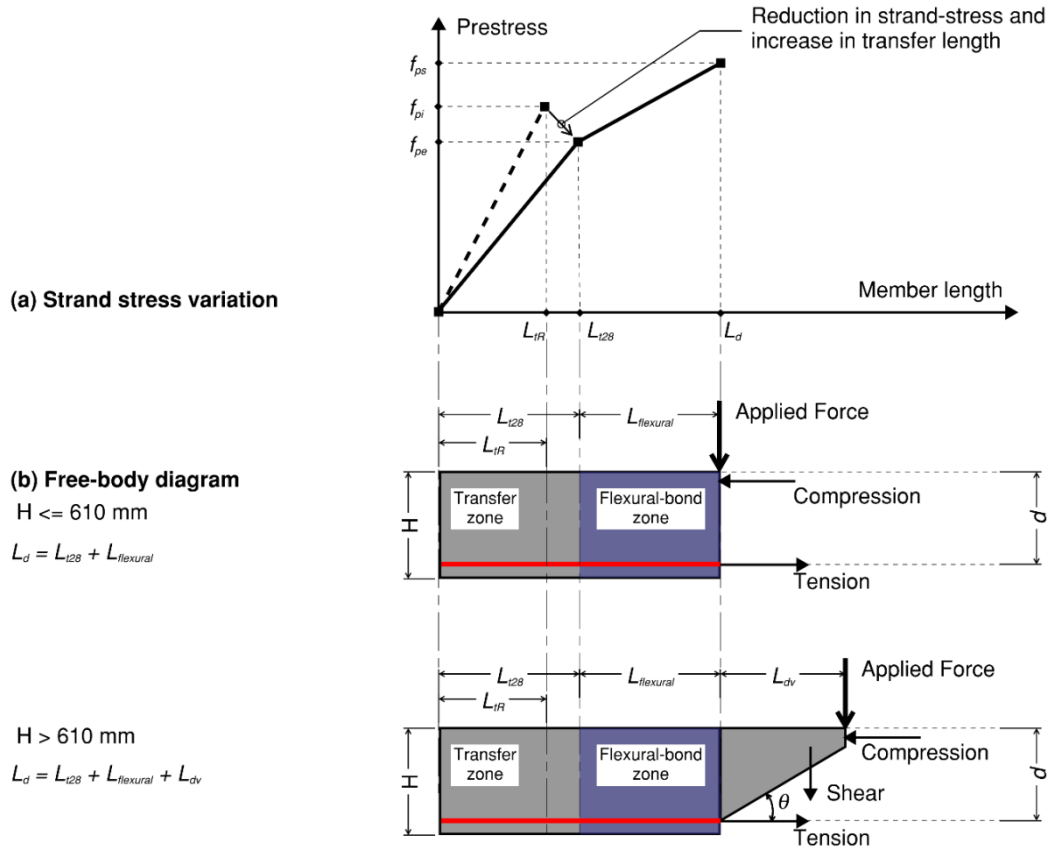


Fig. 5 (a) Strand stress variation in transfer zone and flexural-bond zone; (b) Free-body diagram for a PC member (after Shahawy 2001)

MPa” was the average mortar strength measured during the STSB tests of 12 strand samples. The exponent “0.75” is adopted from Morcouc *et al.* (2012) as the researchers determined this exponent value provides the best fit for the relationship between the measured STSB pullout force and concrete strength. Fig. 2 and Fig. 3 show the similarity of the bond strength values calculated from the simplified and alternative equations. In design, if the concrete strength of the PC members is unknown, the use of the simplified equations is preferable. Otherwise, the use of alternative equations is recommended.

A free-body diagram and strand stress variation at the end of a PC member are shown in Fig. 5. In Fig. 5(a), at release, the transfer length and strand stress are L_{IR} and f_{pi} , respectively. Under the effect of concrete creep and shrinkage (in both transverse and longitudinal directions in relation to the beam’s axial axis), the transfer length increases to L_{I28} while the strand stress decreases to f_{pe} at 28 days of age. If the PC member is externally loaded, a flexural-bond length is required for the development of strand stress f_{ps} . For PC members with a depth greater than 610 mm, Shahawy (2001) recommended an additional shear length (L_{dv}) as visually illustrated in Fig. 5(b) to prevent a shear crack from interrupting the strand-stress development in the flexural-bond zone. The most critical shear crack is assumed to be 30° (θ), developed from the end of the flexural-bond zone. With an approximate effective depth (d)

of $0.85H$, L_{dv} is $1.47H$ as shown in Eq. (7); where H is the depth of PC members.

$$L_{dv} = d \times \cot(\theta) = 0.85H \times \cot(30^\circ) = 1.47H \quad (7)$$

The required development length additionally includes the shear length L_{dv} , along with the transfer length (L_{I28}) and flexural-bond length ($L_{flexural}$). If the depth of the PC members is less than or equal to 610 mm, L_{dv} is not needed. For MC 2010 and EC2, there is no specification regarding the member depth.

The design applications of MC 2010 and EC2 have specific bond equations for the transmission and anchorage zones and at different prestress states. The derived bond equations, Eqs. (5e)-(5f)-(5g) for EC2 and Eqs. (6d)-(6e)-(6f) for MC 2010, can be compared to Eqs. (8)-(9)-(10) in Table 6, respectively. Alternatively, the proposed bond-strength equations can be used to compute the transmission lengths and anchorage length, then compare to the code-predicted values.

5.3.1 Design example 1

The same the prestressing strand tested in this study (with $P_{final} = 161.3$ kN, $P_{initial} = 0.8 \times P_{final} = 0.8 \times 161.3$ kN = 129.0 kN, and $f_{b,STSB} = 4.26$ MPa on average) is used to cast two PC beams (PC1 with 400 mm depth and PC2 with 1100 mm depth), and both beams are cast with the H-SCC mixture ($f'_{ci} = 54.6$ MPa and $f'_c = 73.8$ MPa as presented in

Table 6 Proposed bond strength equations

Zone and prestress stage ^[a]	Simplified equation	Alternative equation	Eq.
Transfer zone at release	$1.25 \times f_{b,STSB}$	$f_{b,STSB} + 0.25 \times f_{b,STSB} \left(\frac{f'_{ci}}{32 \text{ MPa}} \right)^{0.75}$	(8)
Transfer zone at 28 days of age	$1.05 \times f_{b,STSB}$	$f_{b,STSB} + 0.05 \times f_{b,STSB} \left(\frac{f'_c}{32 \text{ MPa}} \right)^{0.75}$	(9)
Flexural-bond zone	$0.8 \times f_{b,STSB}$	$0.8 \times f_{b,STSB}$	(10)

^[a] = refer to Fig. 6 for the location of transfer zone and flexural-bond zone.

Table 2). The prestressing strand is tensioned to 75% of the nominal ultimate strength ($f_{pj} = 1395$ MPa). The total short- and long-term prestress losses are assumed to be 10% and 20% of the initial tensioning stress that are equivalent to 139.6 and 279.2 MPa, respectively.

Using the proposed bond strength equations in Table 6 for PC1, and introducing the corresponding bond strength values in Eqs. (4c)-(4d), the resulting transfer length at release, transfer length at 28 days of age, flexural-bond length, and development length are 560 mm ($32d_b$), 620 mm ($35d_b$), 540 mm ($31d_b$), and 1160 mm ($66d_b$), respectively. For PC2, the transfer length at release and 28 days of age and flexural-bond length are identical to those of PC1. The development length additionally includes the shear length L_{dv} of 1620 mm ($91d_b$), resulting in a development length of 2780 mm ($157d_b$), which is equal to the ACI 318-19 predicted value [2780 mm ($157d_b$)], and less than the AASHTO-LRFD predicted development length [4450 mm ($251d_b$)]. In summary, ACI 318-19 and AASHTO-LRFD adequately predict all of these design parameters for PC1 and PC2.

In addition, both EC2 and MC 2010 provide an adequate prediction for the transmission lengths and anchorage length [for EC2: $L_{tR} = 550$ mm ($31d_b$), $L_{t28} = 830$ mm ($47d_b$), $L_{flexural} = 930$ mm ($52d_b$), and $L_d = 1760$ mm ($99d_b$) for PC1 and 3380 mm ($190d_b$) for PC2; for MC 2010: $L_{tR} = 460$ mm ($26d_b$), $L_{t28} = 920$ mm ($52d_b$), $L_{flexural} = 930$ mm ($52d_b$), and $L_d = 1850$ mm ($104d_b$) for PC1 and 3470 mm ($195d_b$) for PC2].

5.3.2 Design example 2

The H-SCC mixture is used to cast 2 PC beams with the same sections as above. The 18-mm prestressing strand, however, has a lower STSB pullout force of 78.7 kN ($P_{initial}$) and 97.9 kN (P_{final}), as reported in Morcouc *et al.* (2012). In this case, $f_{b,STSB}$ is equal to 2.61 MPa.

The predicted transfer length at release is 910 mm ($52d_b$), which is 12% greater than the measured value of 810 mm ($46d_b$) (Morcouc *et al.* 2014). The predicted transfer length at 28 days of age is 1020 mm ($58d_b$), which is about 12% greater than the measured value of 910 mm ($52d_b$) at 14 days of age – this assumes that the transfer length at 14 days is similar to that at 28 days of age. The predicted transfer length at 28 days of age is slightly longer than the one predicted by ACI 318-19 [1020 mm ($58d_b$) vs.

960 mm ($54d_b$)]. This code adequately predicts the development length of PC1 [1900 mm ($107d_b$) vs. 2780 mm ($157d_b$)], and under-estimates the development length of PC2 [3520 mm ($198d_b$) vs. 2780 mm ($157d_b$)]. Alternatively, AASHTO-LRFD adequately predicts the development length of PC2 [3520 mm ($198d_b$) vs. 4450 mm ($251d_b$)].

On the other hand, EC2 and MC 2010 provide a conservative prediction for the transmission length at release, and under-estimate it at 28 days of age, by 19% to 28%. For the anchorage length, both codes show an under-estimation of 5% to 12%. It should be noted that the code-estimated transmission lengths and anchorage lengths from EC2 and MC 2010 are identical to the respective ones on the design example 1 since the concrete properties are the same.

6. Conclusions

Based on the investigation, the following conclusions were made:

- STSB is a pullout test that can be used to evaluate the bond of prestressing strand. The derived test results provide new insights regarding the bond behavior of prestressing strand in pretensioned concrete members.
- For the mixtures examined in this study, there is minimal difference in strand bond between conventional concrete or self-consolidating concrete.
- The contribution of the Hoyer's effect on the bond of prestressing strand in the transfer zone of PC members can be quantified by subtracting the bond performance determined by the STSB to the bond performance determined from the entire transfer length.
- The contribution of mechanical interlock to the bond of prestressing strand in the flexural-bond zone can be quantified by subtracting the reduction in bond caused by Poisson's effect and the potentially damaged concrete from the bond performance determined by the STSB. A reduction of 20% is determined based on the obtained experimental results.
- Two simplified equations are proposed to quantify strand-bond parameters for the transfer zone. In addition, alternative equations are proposed for determining strand-bond with consideration of concrete compressive strength.

The proposed Eq. (8) is applicable for determining transfer length (or transmission length) at release. This equation is useful because a short transfer length can result in excessive stresses at release. The proposed Eq. (9) is applicable for determining transfer length in service (when the moment and shear capacity are considered), because a long transfer length is critical to these design parameters.

- One simplified equation is proposed to quantify the strand-bond parameter for the flexural-bond zone. The proposed Eq. (10) is applicable for predicting the flexural-bond length, without an interruption in strand-stress development due to shear cracks.

- Two typical design examples highlight the effect of strand bond, representative by STSB pullout force, to the code-established design parameters, such as transfer and development length. The code-predictions can be unconservative for prestressing strands having a low STSB pullout force.

This study investigated the bond mechanisms of prestressing strand in pretensioned concrete members, with an emphasis on conventional and self-consolidating concrete, having compressive strengths of 41 to 68 MPa and 64 to 93 MPa at 1-day and 28-day of age, respectively. Additional research is needed for pretensioned concrete members cast with different types of concrete (i.e., light-weight concrete, high-performance concrete, etc.). In addition, a gradual release technique used in this study did not create a wave of energy that is transferred from prestressing strands to the pretensioned concrete member which can damage the strand bond in the transfer zone. A sudden release technique can generate this energy wave. For small-size members, the generated energy can damage the strand bond. For full-size members, the energy can be absorbed by the concrete mass. The effect of a sudden release technique should be further examined.

Acknowledgements

This research is supported by the University of Arkansas at Fayetteville and the Ton Duc Thang University. The authors would like to thank Insteel Industries Inc. for providing the strands for this research. The authors also would like to thank a number of individuals at the University of Arkansas for their contribution in this study.

References

- AASHTO (2017), *Load and Resistance Factor Design for Highway Bridges Specifications (AASHTO-LRFD)*, American Association of State Highway and Transportation Officials; Washington D.C., USA.
- Abdelatif, A.O., Owen, J.S. and Hussein, M.F. (2015), "Modelling the prestress transfer in pre-tensioned concrete elements", *Finite Elem. Anal. Des.*, **94**, 47-63. <https://doi.org/10.1016/j.finel.2014.09.007>.
- Abrishami, H.G. and Mitchell, D. (1993), "Bond characteristics of pretensioned strand", *ACI Mat. J.*, **90**(3), 228-235.
- ACI (2019), *Building Code Requirements for Structural Concrete and Commentary (ACI 318-19)*, American Concrete Institute; Farmington Hills, MI, USA.
- Arab, A.A., Badie, S.S. and Manzari, M.T. (2011), "A methodological approach for finite element modeling of pretensioned concrete members at the release of pretensioning", *Eng. Struct.*, **33**(6), 1918-1929. <https://doi.org/10.1016/j.engstruct.2011.02.028>.
- ASTM (2015), *Standard Test Method for Evaluating Bond of Seven-Wire Steel Prestressing Strand (ASTM A1081)*, American Society for Testing and Materials; West Conshohocken, PA, USA.
- ASTM (2018), *Standard Specification for Steel Strand, Uncoated Seven-Wire for Prestressed Concrete (ASTM A416)*, American Society for Testing and Materials; West Conshohocken, PA, USA.
- Bai, F. and Davidson, J.S. (2016), "Composite beam theory for pretensioned concrete structures with solutions to transfer length and immediate prestress losses", *Eng. Struct.*, **126**, 739-758. <https://doi.org/10.1016/j.engstruct.2016.08.031>.
- Balazs, G.L. (1992), "Transfer control of prestressing strands", *PCI J.*, **37**(6), 60-71.
- Barakat, S., Al-Toubat, S., Leblouba, M. and Al Burai, E. (2019), "Behavioral trends of shear strengthened reinforced concrete beams with externally bonded fiber-reinforced polymer", *Struct. Eng. Mech.*, **69**(5), 579-589. <https://doi.org/10.12989/sem.2019.69.5.579>.
- Barnes, R.W., Grove, J.W. and Burns, N.H. (2003), "Experimental assessment of factors affecting transfer length", *ACI Struct. J.*, **100**(6), 740-748.
- Briere, V., Harries, K.A., Kasan, J. and Hager, C. (2013), "Dilation behavior of seven-wire prestressing strand-The Hoyer effect", *Constr. Build. Mater.*, **40**, 650-658. <https://doi.org/10.1016/j.conbuildmat.2012.11.064>.
- Buckner, C.D. (1995), "A review of strand development length for pretensioned concrete members", *PCI J.*, **40**(2), 84-99.
- Caro, L., Marti-Vargas, J.R. and Serna, P. (2013), "Time-dependent evolution of strand transfer length in pretensioned prestressed concrete members", *Mech. Time-Depend. Mat.*, **17**(4), 501-527. <https://doi.org/10.1007/s11043-012-9200-2>.
- CEN (2004), *Eurocode 2: Design of Concrete Structures: Part 1-1: General Rules and Rules for Buildings (EC2)*, European Committee for Standardization; Brussels, Belgium.
- Dang, C.N., Floyd, R.W., Hale, W.M. and Marti-Vargas, J.R. (2016a), "Measured development lengths of 0.7 in. (17.8 mm) strands for pretensioned beams", *ACI Struct. J.*, **113**(3), 525-535.
- Dang, C.N., Floyd, R.W., Hale, W.M. and Marti-Vargas, J.R. (2016b), "Measured transfer lengths of 0.7 in. (17.8 mm) strands for pretensioned beams", *ACI Struct. J.*, **113**(1), 85-94.
- Dang, C.N., Floyd, R.W., Murray, C.D., Hale, W.M. and Marti-Vargas, J.R. (2015), "Bond stress-slip model for 0.6 in. (15.2 mm) diameter strand", *ACI Struct. J.*, **112**(5), 625-634.
- Dang, C.N., Murray, C.D., Floyd, R.W., Hale, W.M. and Marti-Vargas, J.R. (2014a), "Analysis of bond stress distribution for prestressing strand by Standard Test for Strand Bond", *Eng. Struct.*, **72**, 152-159. <https://doi.org/10.1016/j.engstruct.2014.04.040>.
- Dang, C.N., Murray, C.D., Floyd, R.W., Hale, W.M. and Marti-Vargas, J.R. (2014b), "A correlation of strand surface quality to transfer length", *ACI Struct. J.*, **111**(5), 1245-1252.
- Den Uijl, J.A. (1998), "Bond modelling of prestressing strand", *ACI Special Publication*, **180**, 145-170.
- FIB (2013), *Model Code for Concrete Structures 2010 (MC 2010)*, International Federation for Structural Concrete; Lausanne, Switzerland.
- Janney, J.R. (1954), "Nature of bond in pre-tensioned prestressed concrete", *ACI J.*, **25**(9), 717-737.
- Jiang, X., Cabage, J., Jing, Y., Ma, Z. J. and Burdette, E.G. (2017), "Effect of embedment length on bond of 18 mm (0.7 in.) strand

- by pullout test”, *ACI Struct. J.*, **114**(3), 707-717.
- Kareem, R.S., Al-Mohammed, A., Dang, C.N., Martí-Vargas, J.R. and Hale, W.M. (2019), “Bond model of 15.2-mm strand with consideration of concrete creep and shrinkage”, *Mag. Concr. Res.*, 799-810. <https://doi.org/10.1680/jmacr.18.00506>.
- Lee, C., Lee, S. and Shin, S. (2017), “Modeling of transfer region with local bond-slip relationships”, *ACI Struct. J.*, **114**(1), 187-196.
- Llau, A., Jason, L., Dufour, F. and Baroth, J. (2016), “Finite element modelling of 1D steel components in reinforced and prestressed concrete structures”, *Eng. Struct.*, **127**, 769-783. <https://doi.org/10.1016/j.engstruct.2016.09.023>.
- Martí-Vargas, J.R., Arbelaez, C.A., Serna-Ros, P., Navarro-Gregori, J. and Pallares-Rubio, L. (2007), “Analytical model for transfer length prediction of 13 mm prestressing strand”, *Struct. Eng. Mech.*, **26**(2), 211-229. <https://doi.org/10.12989/sem.2007.26.2.211>.
- Martí-Vargas, J.R., Caro, L.A. and Serna, P. (2014a), “Size effect on strand bond and concrete strains at prestress transfer”, *ACI Struct. J.*, **111**(2), 419-429.
- Martí-Vargas, J.R., García-Taengua, E., Caro, L.A. and Serna, P. (2014b), “Measuring specific parameters in pretensioned concrete members using a single testing technique”, *Measurement*, **49**, 421-432. <https://doi.org/10.1016/j.measurement.2013.12.007>.
- Martí-Vargas, J.R., García-Taengua, E. and Serna, P. (2013), “Influence of concrete composition on anchorage bond behavior of prestressing reinforcement”, *Constr. Build. Mater.*, **48**, 1156-1164. <https://doi.org/10.1016/j.conbuildmat.2013.07.102>.
- Martí-Vargas, J.R., Hale, W.M., García-Taengua, E. and Serna, P. (2014c), “Slip distribution model along the anchorage length of prestressing strands”, *Eng. Struct.*, **59**, 674-685. <https://doi.org/10.1016/j.engstruct.2013.11.032>.
- Mitchell, D., Cook, W.D., Khan, A.A. and Tham, T. (1993), “Influence of high strength concrete on transfer and development length of pretensioning strand”, *PCI J.*, **38**(3), 52-66.
- Morcous, G., Assad, S., Hatami, A. and Tadros, M.K. (2014), “Implementation of 0.7 in. diameter strands at 2.0× 2.0 in. spacing in pretensioned bridge girders”, *PCI J.*, **59**(3), 145-158.
- Morcous, G., Hatami, A., Maguire, M., Hanna, K. and Tadros, M. (2012), “Mechanical and Bond properties of 18-mm- (0.7-in.-) diameter prestressing strands”, *J. Mat. Civil Eng.*, **24**(6), 735-744. [https://doi.org/10.1061/\(ASCE\)MT.1943-5533.0000424](https://doi.org/10.1061/(ASCE)MT.1943-5533.0000424).
- Motwani, P. and Laskar, A. (2019), “Influence of excessive end slippage on transfer length of prestressing strands in PC members”, *Structures*, **20**, 676-688. <https://doi.org/10.1016/j.istruc.2019.05.004>.
- Moustafa, S.E. (1974), “Pull-out strength of strand and lifting loops”, Research Report No. 74-B5; Concrete Technology Associates, Tacoma, WA, USA.
- Myers, J.J., Volz, J.S., Sells, E., Porterfield, K., Looney, T., Tucker, B. and Holman, K. (2012), “Report B: Self-Consolidating Concrete (SCC) for infrastructure elements: bond, transfer length and development length of prestressing strand in SCC”, Research Report No. CMR 13-003 (Report B); Missouri Department of Transportation, Missouri University of Science and Technology, MO, USA.
- Naji, B., Ross, B.E. and Floyd, R.W. (2016), “Characterization of bond-loss failures in pretensioned concrete girders”, *J. Bridge Eng.*, **22**(4), 1-6. [https://doi.org/10.1061/\(ASCE\)BE.1943-5592.0001025](https://doi.org/10.1061/(ASCE)BE.1943-5592.0001025).
- Oh, B.H., Lim, S.N., Lee, M.K. and Yoo, S.W. (2014), “Analysis and prediction of transfer length in pretensioned, prestressed concrete members”, *ACI Struct. J.*, **111**(6), 1-12.
- Ortega, N.F., Moro, J.M. and Meneses, R.S. (2018), “Theoretical model to determine bond loss in prestressed concrete with reinforcement corrosion”, *Struct. Eng. Mech.*, **65**(1), 1-7. <https://doi.org/10.12989/sem.2018.65.1.001>.
- Osborn, A.E.N., Lawler, J.S. and Connolly, J.D. (2008), “Acceptance tests for surface characteristics of steel strands in prestressed concrete”, Research Report No. NCHRP 621; Transportation Research Board, Washington D.C., USA.
- Park, H. and Cho, J. (2014), “Bond-slip-strain relationship in transfer zone of pretensioned concrete elements”, *ACI Struct. J.*, **111**(3), 503-514.
- Ramirez, J.A. and Russell, B.W. (2008), “Transfer, development and splice length for strand/reinforcement in high strength concrete”, Research Report No. NCHRP 603; Transportation Research Board, Washington D.C., USA.
- Ramirez-Garcia, A.T., Dang, C.N., Hale W.M. and Martí-Vargas, J.R. (2017), “A higher-order equation for modeling strand bond in pretensioned concrete beams”, *Eng. Struct.*, **131**, 345-361. <https://doi.org/10.1016/j.engstruct.2016.10.050>.
- Riding, K.A., Peterman, R.J. and Polydorou, T. (2016), “Establishment of minimum acceptance criterion for strand bond as measured by ASTM A1081”, *PCI J.*, **61**(3), 86-103.
- Russell, B.W. (2006), “NASP round IV strand bond testing”, Final Report; Oklahoma State University, OK, USA.
- Russell, B.W. and Burns, N.H. (1993), “Design guidelines for transfer, development and debonding of large diameter seven wire strands in pretensioned concrete girders”, Research Report No. FHWA/TX-93+1210-5F; Texas Department of Transportation, Austin, TX, USA.
- Shahawy, M. (2001), “A critical evaluation of the AASHTO provisions for strand development length of prestressed concrete members”, *PCI J.*, **46**(4), 94-117.
- Steensels, R., Vandewalle, L., Vandoren, B. and Degée, H. (2017), “A two-stage modelling approach for the analysis of the stress distribution in anchorage zones of pre-tensioned, concrete elements”, *Eng. Struct.*, **143**, 384-397. <https://doi.org/10.1016/j.engstruct.2017.04.0>.
- Tang, C.W. (2018), “Local bond-slip behavior of medium and high strength fiber reinforced concrete after exposure to high temperatures”, *Struct. Eng. Mech.*, **66**(4), 477-485. <https://doi.org/10.12989/sem.2018.66.4.477>.
- Trejo, D., Hueste, M.B.D., Kim, Y.H. and Atahan, H. (2008), “Characterization of self-consolidating concrete for design of precast, prestressed bridge girders”, Research Report No. FHWA/TX-09/0-5134-2, Transportation Research Board, Washington D.C., USA.
- Van Meirvenne, K., De Corte, W., Boel, V. and Taerwe, L. (2018), “Non-linear 3D finite element analysis of the anchorage zones of pretensioned concrete girders and experimental verification”, *Eng. Struct.*, **172**, 764-779. <https://doi.org/10.1016/j.engstruct.2018.06.065>.
- Warenycia, K., Diaz-Arancibia, M. and Okumus, P. (2017), “Effects of confinement and concrete nonlinearity on transfer length of prestress in concrete”, *Structures*, **11**, 11-21. <https://doi.org/10.1016/j.istruc.2017.04.002>.
- Yapar, O., Basu, P. and Nordendale, N. (2015), “Accurate finite element modeling of pretensioned prestressed concrete beams”, *Eng. Struct.*, **101**, 163-178. <https://doi.org/10.1016/j.engstruct.2015.07.018>.

CC

Notations

Concrete member:

H = depth of pretensioned concrete member, mm

d = effective depth of pretensioned concrete member, mm

θ = most critical shear crack, assumed to be 30°

Concrete material:

f'_{ci} = concrete compressive strength at release, MPa

f'_c = concrete compressive strength at 28 days, MPa

$f_{ctd,R}$ = design concrete tensile strength at release, MPa

$f_{ctd,28}$ = design concrete tensile strength at 28 day, MPa

Prestressing strand:

d_b = diameter of prestressing strand, mm

A_p = cross-sectional area of prestressing strand ($7/36 \cdot \pi d_b^2$), mm²

C_p = perimeter of prestressing strand ($4/3 \cdot \pi d_b$), mm

f_p = stress in prestressing strand, MPa

f_{pj} = tensioning stress, MPa

f_{pi} = initial prestress (just after release), MPa

f_{pe} = effective prestress (after all losses), MPa

f_{ps} = stress in prestressing strand at the nominal flexural strength of the PC member, MPa

Bond parameters in pretensioned concrete members:

$L_{embedment}$ = embedment length of prestressing strand, mm

L_t = transfer length (or transmission length), mm

L_{tR} = transfer length at release, mm

L_{t28} = transfer length at 28 days of age, mm

$L_{flexural}$ = flexural-bond length, mm

L_{dv} = shear length, mm

L_d = development length (or anchorage length) when the moment and shear capacity are considered, mm

f_b = prestressing strand-to-concrete bond stress, MPa

Standard Test for Strand Bond (STSB):

$P_{initial}$ = pullout force corresponding to a free-end slip of 0.25 mm, kN

P_{final} = pullout force corresponding to a free-end slip of 2.5 mm, kN

$f_{b,STSB}$ = bond strength obtained in the STSB, MPa

Eurocode 2:

α_1 = coefficient of release techniques (1.0 for gradual release and 1.25 for sudden release)

α_2 = strand area factor (0.19 for 7-wire strands)

η_1 = coefficient of strand bond conditions (1.0 for good bond conditions and 0.7 otherwise)

η_{p1} = coefficient accounting for the type of tendon and bond situation in the transfer zone (3.2 for 7-wire strands)

η_{p2} = coefficient accounting for the type of tendon and bond situation in the flexural bond zone (1.2 for 7-wire strands)

σ_{pi} = prestress just after release (equivalent to f_{pi}), MPa

σ_{pe} = effective prestress (equivalent to f_{pe}), MPa

σ_{pd} = strand stress under design load (equivalent to f_{ps}), MPa

f_{bpt} = design bond strength within the transfer zone at prestress transfer state, MPa

f_{bpd} = design bond strength in the flexural bond zone in the ultimate limit state, MPa

Model Code for Concrete Structures 2010:

α_{p1} = coefficient of release techniques (1.0 for gradual release and 1.25 for sudden release)

α_{p2} = coefficient of design state to be verified (0.5 at release

and 1.0 at service when the moment and shear capacity is considered)

α_{p3} = coefficient of strand bond situations (0.7 for intended wires and 0.5 for 7-wire strands)

η_{p1} = coefficient of type of tendon (1.2 for 7-wire strands)

η_{p2} = coefficient of tendon position (1.0 for all tendons with an inclination of 45° to 90° with respect to the horizontal during concreting and for all horizontal tendons which are up to 250 mm from the bottom or at least 300 mm below the top of the concrete section during concreting, and 0.7 for all other cases)

σ_{pi} = prestress just after release (equivalent to f_{pi}), MPa

σ_{pe} = effective prestress (equivalent to f_{pe}), MPa

σ_{pd} = strand stress under design load (equivalent to f_{ps}), MPa

f_{bpd} = design bond strength, MPa

f_{ctd} = design concrete tensile strength, MPa

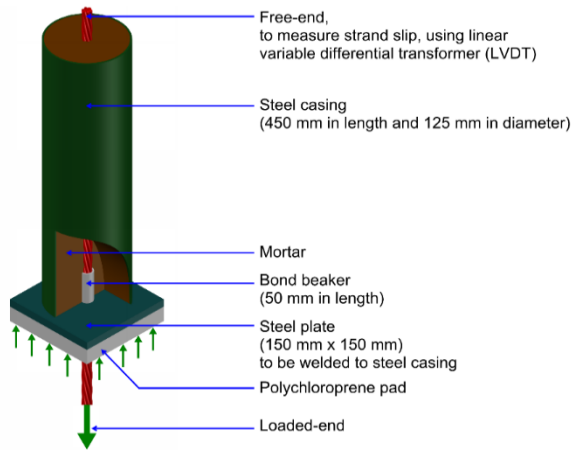


Fig. A1 STSB test setup

Appendix 1: Standard Test for Strand Bond (STSB)

A STSB test setup is shown in Fig. A1. The sample is placed in a steel frame, which has a setup similar to the one ASTM A1081 (ASTM 2015) recommended. A linear variable differential transformer was used to measure strand slip at the free-end. A force with a displacement rate of (2.54 mm/min \pm 0.0127 mm/min) was applied at the loaded-end. A data acquisition system was used to record the strand slip and pullout force continuously. The test stops as the strand slip exceeds 2.5 mm. In this study, the STSB tests continued until the strand slip reached 3.5 mm.

Appendix 2: Measurement of transfer length

The demountable mechanical (DEMEC) strain gauges used to measure the concrete strains are shown in Fig. A2. DEMEC target points were attached to the beam surface at the same level of prestressing strands, at a 100-mm spacing. The determination of transfer length can be nominally divided into 5 steps as below. Fig. A3 illustrates the transfer-length determination using these 5 steps for the live end of the first beam in the H-CC group.

Step 1: Plot the concrete strain profile along the beam length.

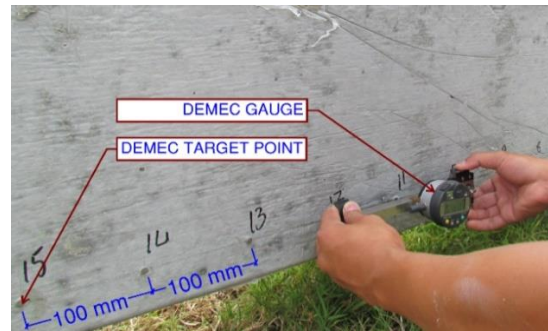


Fig. A2 Concrete strain measurement

Step 2: Determine the constant strain plateau to calculate the average maximum strain (AMS) value.

Step 3: Draw the 95% AMS line. This is the horizontal line passing through the 95% AMS value which accounts for the Saint-Venant's effect associated to the prestress transfer phenomenon.

Step 4: Draw the initial-linear trend (ILT) line. The ILT line passes through the origin and is the best-fit trend line of target points within the transfer zone. The ILT line represents the linear strand stress in the transfer zone. The advantage of using the ILT line is to reduce the effect of strain fluctuation near the end of the transfer zone and to provide more precise and consistent measurements.

Step 5: Determine the intersection of the 95% AMS line and the ILT line. Transfer length is the distance from the beam end to the intersection point.

Appendix 3: Measurement of development length

There were two flexure tests for each beam; one at the dead end and the other one at the live end. Fig. A4 shows a typical setup for a flexure test. A data acquisition system was used to continuously monitor the variation of strand slip, applied force, and beam deflection. A linear variable differential transformer was used to monitor strand slip. A linear cable encoder was used to record the beam deflection at the applied force location. The test data were then transferred and stored in a computer for analysis of failure modes. The cracking pattern was photographed using a digital camera and visualized in a 2D computer-aided design software.

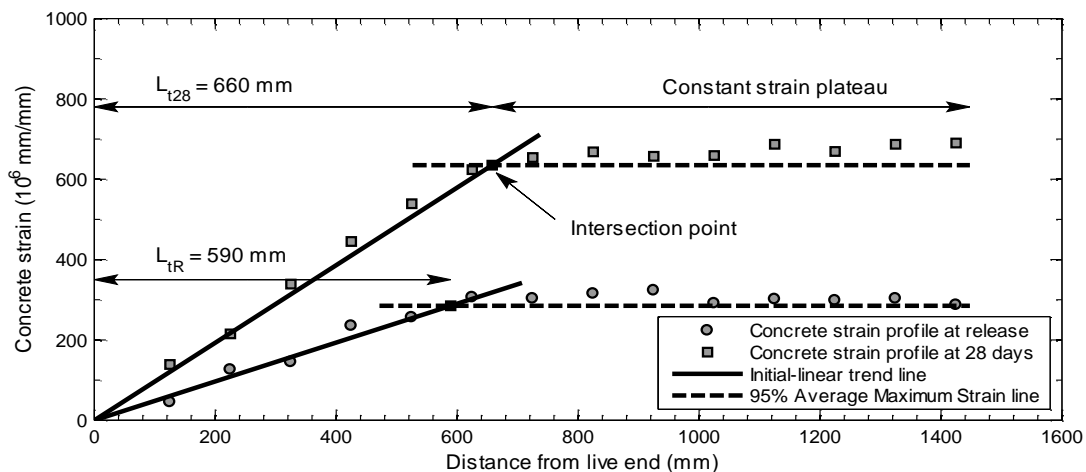


Fig. A3 Transfer lengths at the live end of the first beam in H-CC group

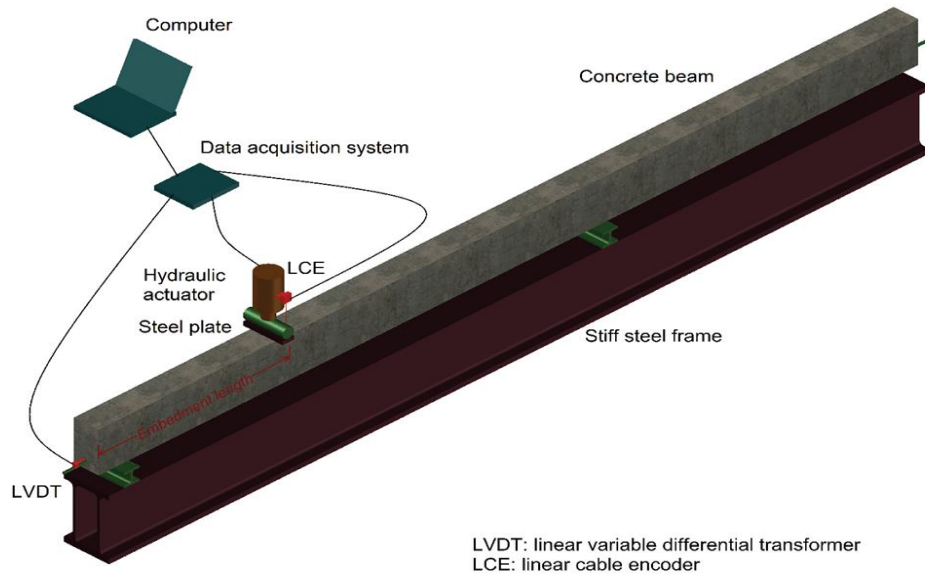


Fig. A4 Bending test setup for development-length determination.